Progress In Electromagnetics Research Letters, Vol. 90, 143–149, 2020

Compact Balanced Bandpass Filter with High Selectivity Based on Two Coupled Dual-Mode Microstrip Loop Resonators

Xiao-Bang Ji[1] and Mi Yang[2, *]

Abstract—This letter proposes a novel single-layer fourth-order balanced bandpass filter based on two coupled dual-mode loop resonators. Two pairs of balanced input/output (IO) feeding lines with unequal arms are employed to excite the outside dual-mode loop resonator, and the inside dual-mode loop resonator with meander lines is coupled to the outside one. Under differential-mode (DM) operation, three finite transmission zeros (FTZs) can be produced and controlled. Under common mode (CM) operation, the rejection level can be controlled by the length of IO feeding arms. For the demonstration, a balanced dual-mode loop filter with the center frequency of 5.2 GHz is designed, fabricated, and measured. The proposed balanced filter has the advantages of compact size, high selectivity, wide stopband of DM response, and good CM suppression.

1. INTRODUCTION

Balanced microstrip bandpass filters (BPFs) have the advantages of compact size, light weight, and low cost, which have more advantages than unbalanced microstrip bandpass filters due to their high immunity to the environmental noises, good dynamic range, and low electromagnetic interference (EMI) in communication systems [1–6]. Moreover, dual-mode microstrip loop resonator can be employed to design balanced filters with high performance [7–10]. In [7], a balanced dual-mode loop bandpass filter was proposed and designed, and a dual-mode loop resonator with capacitive-loaded arms was employed to realize compact size, but only two transmission poles of the balanced filter in [7] can be realized. Moreover, the balanced filter in [7] has poor performances of selectivity and stopband rejection. In [8–10], balanced microstrip filters are designed by using a dual-mode loop combined with single-mode microstrip-line resonators. Because the balanced filters in [8–10] can realize fourth-order differential mode (DM) responses, high selectivity of DM response and wideband common mode (CM) suppression can be achieved. However, their sizes are large.

This letter proposes a novel single-layer fourth-order balanced bandpass filter based on two coupled dual-mode loop resonators to realize a high-performance balanced filter with a reduced size. Two pairs of balanced input/output (IO) feeding lines with unequal arms are employed to excite the outside dual-mode loop resonator, and the inside dual-mode loop resonator with meander lines is coupled to the outside one. The proposed dual-mode loop filter can be equivalent to a dual-extended doublet coupling scheme without source-load (S-L) coupling. Under differential-mode (DM) operation, three finite transmission zeros (FTZs) can be produced and controlled. Under common mode (CM), the rejection level can be controlled by the length of IO feeding arms. For the demonstration, a fourth-order balanced dual-mode loop filter with the center frequency of 5.2 GHz is designed, fabricated and measured.

Received 17 January 2020, Accepted 5 March 2020, Scheduled 27 April 2020

* Corresponding author: Mi Yang (794781930@qq.com).

[1] School of Electrical Engineering, Henan Polytechnic, Zhengzhou 450046, China. [2] Department of Electromagnetic Wave and Antenna Propagation, China Huayin Ordnance Test Center, Huayin, Shaanxi 714200, China.

2. THE PROPOSED BALANCED DUAL-MODE LOOP MICROSTRIP FILTER

2.1. The Proposed Balanced Filter

Top view of the proposed balanced dual-mode microstrip loop filter is shown in Fig. 1(a). It is composed of two dual-mode loop resonators and two pairs of balanced feeding lines. The proposed balanced filter is symmetric about the diagonal line T_1T_2. The balanced input ports are denoted by S_1 and S_2, respectively. Balanced output ports are denoted by L_1 and L_2, respectively. Two pairs of balanced input/output (IO) feeding lines with unequal arms are employed to excite the outside dual-mode loop resonator. Locations of IO ports can be deviated from the center of loop resonator, and the deviated distance is denoted by D_{in}.

The inside dual-mode loop resonator with meander lines is coupled to the outside loop resonator. Perturbation metal patches, located at the corners of two loop resonators, are employed to split the degenerate modes, and the perturbed two modes are even and odd modes, as shown in Fig. 2. Because the electric-field distributions of the two modes on the balanced input/output ports are out-of-phase, the two modes can be excited by DM signals, and the CM signals cannot be passed through the two modes. Under DM operation, the proposed dual-mode loop filter can be equivalent to a dual-extended doublet

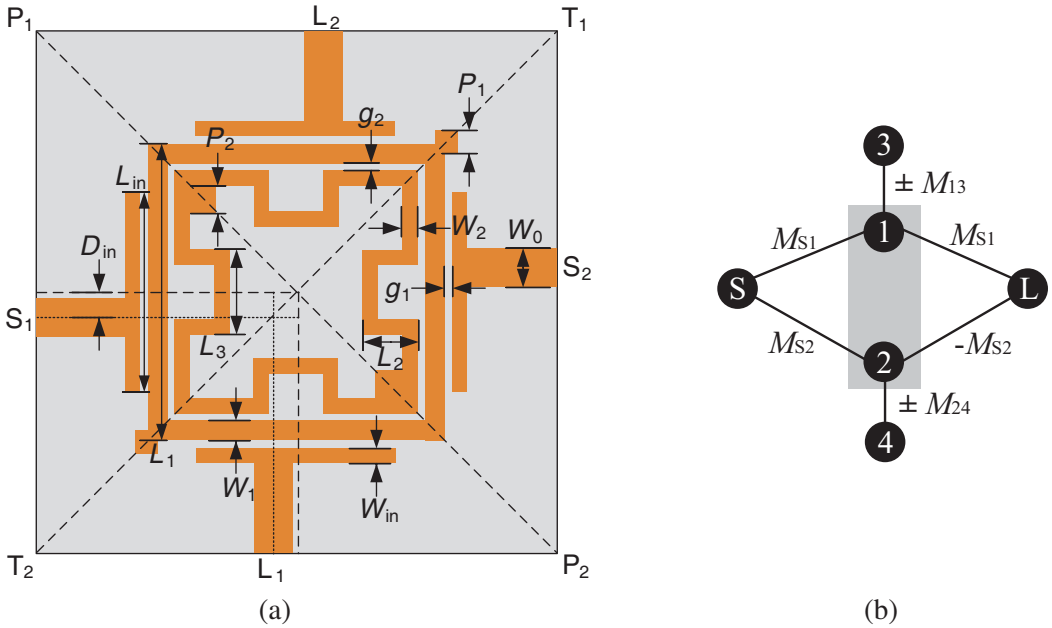

Figure 1. (a) Layout of the proposed balanced dual-mode loop filter, (b) corresponding coupling scheme under DM operation (S/L: source/load, 1/2: even and odd modes in outside loop resonator respectively, 3/4: even and odd modes in inside loop resonator respectively).

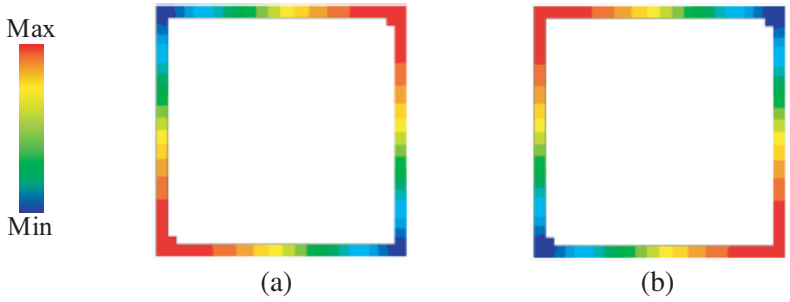

Figure 2. Electric-field distributions of the dual-mode loop resonator. (a) Even mode, (b) odd mode.

coupling scheme without source-load (S-L) coupling, as shown in Fig. 1(b), and thus, three FTZs can be produced. Substrate material of Roger 5880 with its relative permittivity of 2.2 and thickness of 0.508 mm have been used for the design.

2.2. Analysis of the Proposed Balanced Filter

All structures, in this letter, are simulated by HFSS and designed on a dielectric substrate with $\varepsilon_r = 2.2$ and $h = 0.508$ mm. Based on the proposed structure in Fig. 1(a), the external quality factors (Q_e) of the two modes can be controlled well by parameters D_{in} and g_1. Q_e of even and odd modes are denoted by Q_{e1} and Q_{e2}, respectively. A single port structure is used to extract Q_e which can be calculated by using HFSS and the following formula (1) [11]:

$$Q_e = \frac{\omega_0}{\Delta\omega_{\pm 90^\circ}} \tag{1}$$

where ω_0 is the resonance, and $\Delta\omega_{\pm 90^\circ}$ is determined from the resonance at which the phase shifts $\pm 90^\circ$ with respect to the absolute phase at ω_0. The extracted Q_e are shown in Fig. 3(a). When $D_{in} = 0$, Q_e of two modes are almost equal because of their symmetric field distributions. The relationship between external quality factors (Q_{e1} and Q_{e2}) and external coupling coefficients (M_{S1} and M_{S2}) can be expressed as Eq. (2) [11]:

$$Q_{ei} = \frac{1}{M_{Si}^2 \cdot \mathrm{FBW}} \tag{2}$$

where FBW is the fractional bandwidth. When D_{in} is larger or smaller than zero, the external quality factor Q_{e1} can be larger or smaller than Q_{e2}, i.e., M_{S1} is smaller or larger than M_{S2}. Thus, the coupling coefficients M_{S1} and M_{S2} can be controlled well by parameters D_{in} and g_1.

When two even modes of two odd modes with eigen resonances of 5.2 GHz are coupled, two resonant frequencies will be split. The two resonances are denoted by f_1 and f_2. Coupling coefficients can be numerically extracted by using HFSS and the following formula (3) [11]:

$$|k| = \frac{|f_2^2 - f_1^2|}{f_2^2 + f_1^2} \tag{3}$$

As shown in Fig. 3(b), the extracted $|k_{13}|$ of coupling path 1–3 is presented, and $|k_{13}|$ can be controlled well. Similarly, the coupling coefficient $|k_{24}|$ of coupling path 2–4 can also be controlled well, and the extracted results are not presented here. The denormalized coupling coefficient K_{ij} between two coupled modes can be synthesized with the normalized coupling coefficient M_{ij} by Eq. (4) [11]:

$$k_{ij} = \mathrm{FBW} \cdot M_{ij} \tag{4}$$

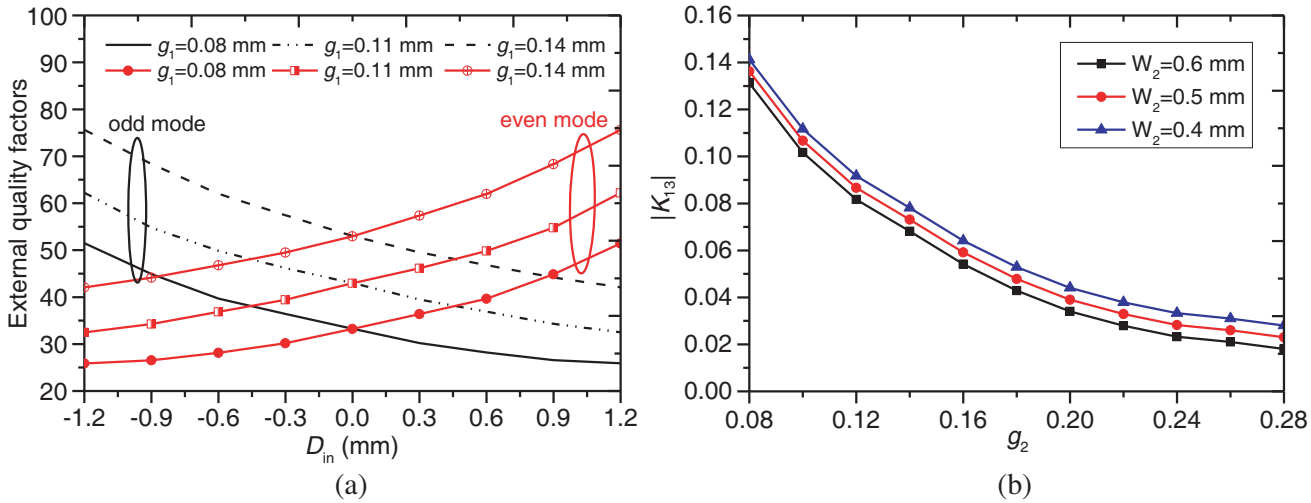

Figure 3. Extracted external quality factors and coupling coefficients at operating frequency of 5.2 GHz. (a) External quality factors, (b) coupling coefficient $|K_{13}|$.

Under DM operation, a quasi-elliptic response with three FTZs can be realized, and locations of FTZs can be controlled well. As shown in Fig. 4(a), when the deviated distance of feeding lines is changed, the third FTZ can be controlled because the location of the third FTZ is decided by the ratio of M_{S1}/M_{S2}. As shown in Fig. 4(b), when the size of the perturbation metal patches on the outside loop resonator is changed, locations of three FTZs are all changed. As shown in Fig. 4(c), when the size of the perturbation metal patches on the inside loop resonator is changed, locations of the first two FTZs are changed. Thus, the three FTZs can be controlled well.

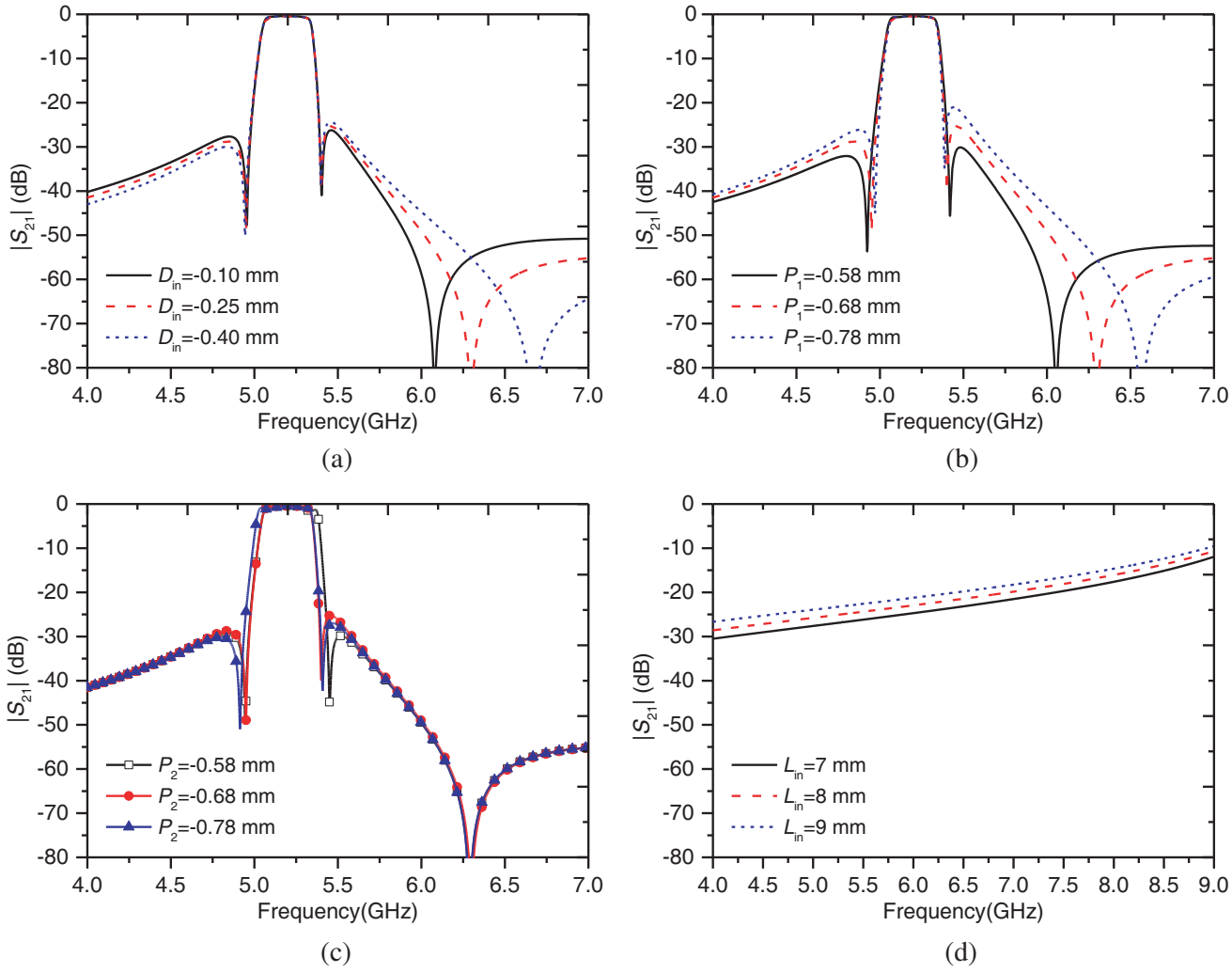

Figure 4. Simulated responses. (a) Controllable FTZs with changing D_{in}, (b) controllable FTZs with changing P_1, (c) controllable FTZs with changing P_2, (d) controllable CM rejection level with changing L_{in}.

Under CM operation, the exciting signals fail to excite the electric field in Fig. 2 because the effects of the two CM exciting signals are canceled out each other. Thus, CM signals cannot be passed through the proposed filter. Thus, the proposed balanced dual-mode filter has the intrinsic features of DM operation and CM suppression. When the length of feeding arms is changed, the CM rejection level can be changed, as shown in Fig. 4(d). The higher-order modes in loop resonator are excited by the CM signals, which can deteriorate the CM rejection level. For the unbalanced dual-mode loop filter, the bypass coupling based on the higher-order modes mainly provides the equivalent S-L coupling.

3. SIMULATED AND MEASURED RESULTS

Based on the proposed balanced dual-mode loop filter in Fig. 1 and the extracted results in Fig. 3, a balanced filter with the DM center frequency (f_{0DM}) of 5.2 GHz, bandwidth of 250 MHz, and return loss (RL) of 20 dB is designed for the demonstration. Three FTZs are located at 4.94, 5.41, and 6.18 GHz. The simulated DM responses are shown in Fig. 5(a), and the synthesized responses based on the equivalent dual-extended doublet coupling scheme in Fig. 1(b) are also plotted in Fig. 5(a) for the comparison with simulated responses. The synthesized and simulated responses are matched well. The corresponding coupling matrix with resonant and non-resonant nodes is shown in Eq. (5). The structure parameters of the designed filter are given as follows: $W_0 = 1.54$, $W_{in} = 0.3$, $L_{in} = 8$, $W_1 = 0.5$, $W_2 = 0.4$, $g_1 = 0.14$, $g_2 = 0.13$, $P_1 = 0.68$, $P_2 = 0.71$, $L_1 = 11.11$, $L_2 = 1.65$, $L_3 = 2.6$ (all units: mm).

$$\begin{bmatrix} & S & 1 & 2 & 3 & 4 & L \\ S & 0 & 0.7320 & 0.7118 & 0 & 0 & 0 \\ 1 & 0.7320 & 0.2221 & 0 & 0.7357 & 0 & 0.7320 \\ 2 & 0.7118 & 0 & -0.1897 & 0 & 0.9704 & -0.7118 \\ 3 & 0 & 0.7357 & 0 & -0.8723 & 0 & 0 \\ 4 & 0 & 0 & 0.9704 & 0 & 0.6782 & 0 \\ L & 0 & 0.7320 & -0.7118 & 0 & 0 & 0 \end{bmatrix} \tag{5}$$

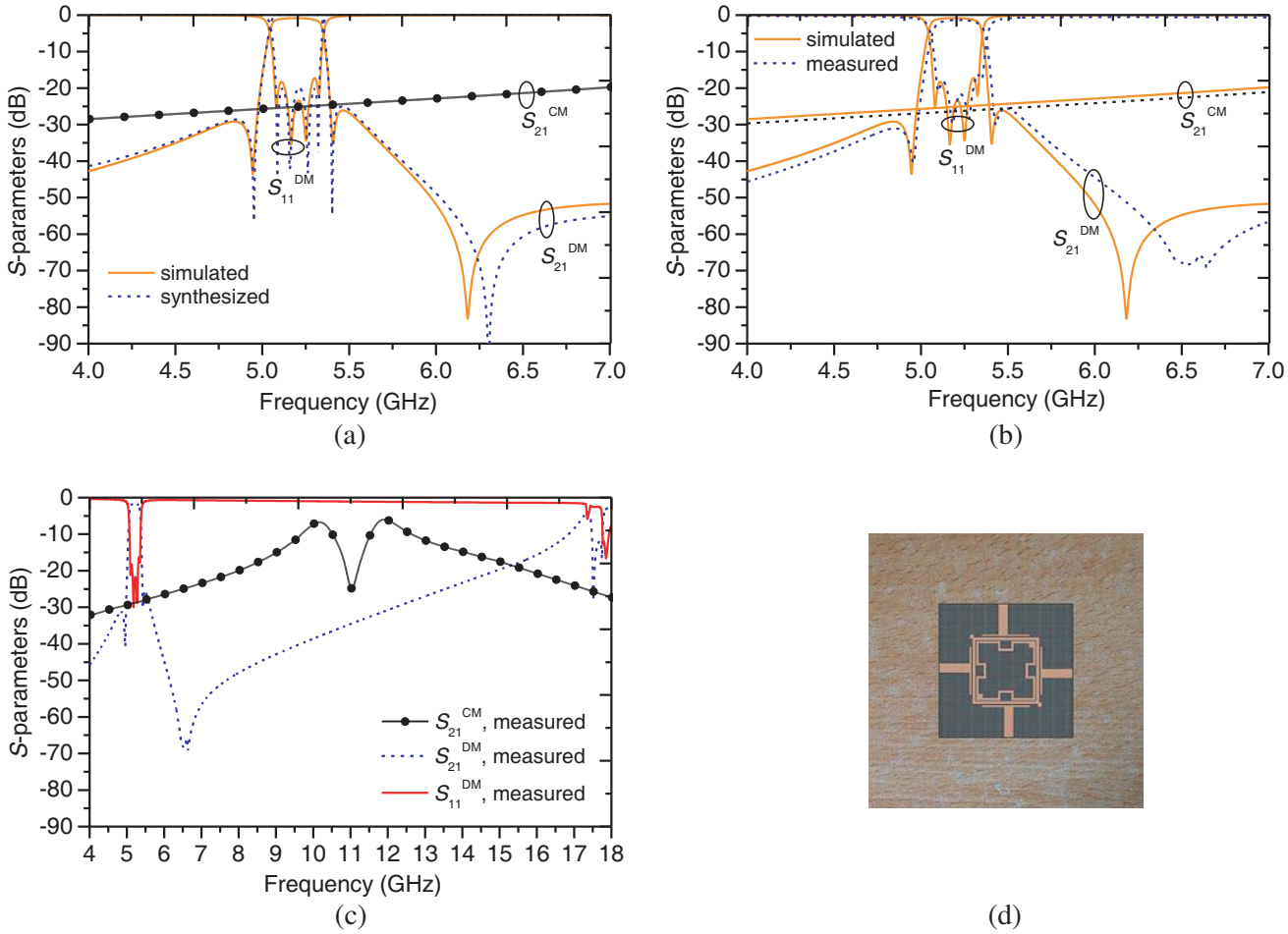

Figure 5. Measured and simulated frequency response of the proposed balanced BPF. (a) Synthesized and simulated DM responses, (b) simulated and measured responses, (c) wideband responses under DM and CM operations, (d) photograph of the fabricated filter.

To verify the designed dual-mode loop filter, the prototype is fabricated and measured. The comparisons between the simulated and measured responses are presented in Fig. 5(b). For the DM responses (S_{21}^{DM} and S_{11}^{DM}), the measured f_{0DM}, insertion loss (IL), minimum return loss (RL), and 3-dB bandwidth are 5.21 GHz, 1.88 dB, 17.14 dB, and 279 MHz (5.1%), respectively. Three FTZs at 4.95, 5.46, and 6.58 GHz can be clearly observed as expected. Wideband responses are shown in Fig. 5(c). Rejection level over 20 dB of DM upper stopband is better than 15 GHz, which indicates that the proposed filter has a wide stopband of DM response. The first spurious passband measured in DM responses (S_{21}^{DM}) appears at about 17.4 GHz (i.e., $3.34f_{0DM}$). For the CM response (S_{21}^{CM}), the rejection level at the f_{0DM} is about 29 dB. Moreover, rejection level over 15 dB is better than 8.93 GHz, which indicates that the proposed filter has a good CM suppression. The first spurious passband measured in CM responses (S_{21}^{CM}) appears at about 10.1 GHz (i.e., $1.94f_{0DM}$), which results in a poor rejection level of CM suppression. The size of the designed filter is about 12 mm × 12 mm ($0.29\lambda_g \times 0.29\lambda_g$), where λ_g is the guided wavelength at f_{0DM}. A photograph of the fabricated filter is shown in Fig. 5(d).

Table 1 provides detailed comparisons with other reported balanced dual-mode loop filters. The proposed balanced dual-mode loop filter can realize compact size and high performance of CM suppression as well as DM response.

Table 1. Compared with other recently reported balanced microstrip filters.

Ref.	f_{0DM} (GHz)	FBW (%)	order	FTZs	Size ($\lambda_g \times \lambda_g$)	DM suppression	In-band CM suppression/dB	CM suppression
[7]	2.39	2.5	2	2	0.21×0.21	33 dB@$2.72f_{0DM}$	24.4	20 dB@$2.71f_{0DM}$
[8]-I	2.395	10.4	4	2	0.63×0.63	20 dB@$1.94f_{0DM}$	42.8	40 dB@$1.78f_{0DM}$
[8]-II	2.38	6.7	4	3	0.63×0.63	40 dB@$4.9f_{0DM}$	48	40 dB@$3.99f_{0DM}$
[9]	2.39	17	3	6	0.64×0.64	15 dB@$2.08f_{0DM}$	18	18 dB@$2.62f_{0DM}$
III	5.22	5.1	4	3	0.29×0.29	30 dB@$2.88f_{0DM}$	29	15 dB@$1.72f_{0DM}$

4. CONCLUSION

In this letter, a novel single-layer balanced microstrip bandpass filter using two coupled loop resonators is proposed. Three FTZs are produced and can be controlled well. The proposed balanced dual-mode loop filter has the advantages of compact size, high selectivity, wide stopband of DM response, and good CM suppression. For demonstration, a balanced dual-mode loop filter is designed, fabricated, and measured. Both the simulated and measured results indicate that the proposed technique can become a competitive candidate for the development of RF/microwave circuits and systems.

REFERENCES

1. Wu, C., C. Wang, and C. H. Chen, "Balanced coupled-resonator bandpass filters using multisection resonators for common-mode suppression and stopband extension," *IEEE Transactions on Microwave Theory and Techniques*, Vol. 55, No. 8, 1756–1763, Aug. 2007.
2. Wu, C., C. Wang, and C. H. Chen, "Novel balanced coupled-line bandpass filters with common-mode noise suppression," *IEEE Transactions on Microwave Theory and Techniques*, Vol. 55, No. 2, 287–295, Feb. 2007.
3. Wu, C., C. Wang, and C. H. Chen, "Stopband-extended balanced bandpass filter using coupled stepped-impedance resonators," *IEEE Microwave and Wireless Components Letters*, Vol. 17, No. 7, 507–509, Jul. 2007.
4. Yan, T., D. Lu, J. Wang, and X. Tang, "High-selectivity balanced bandpass filter with mixed electric and magnetic coupling," *IEEE Microwave and Wireless Components Letters*, Vol. 26, No. 6, 398–400, Jun. 2016.

5. Feng, W. and W. Che, "Novel wideband differential bandpass filters based on t-shaped structure," *IEEE Transactions on Microwave Theory and Techniques*, Vol. 60, No. 6, 1560–1568, Jun. 2012.
6. Shi, J. and Q. Xue, "Balanced bandpass filters using center-loaded half-wavelength resonators," *IEEE Transactions on Microwave Theory and Techniques*, Vol. 58, No. 4, 970–977, Apr. 2010.
7. Gu, H., L. Ge, and L. Xu, "Simple dual-mode balanced bandpass filter with high selectivity and extended common-mode noise suppression," *Electronics Letters*, Vol. 54, No. 13, 833–835, Jun. 28, 2018.
8. Guo, X., L. Zhu, and W. Wu, "A new concept of partial electric/magnetic walls for application in design of balanced bandpass filters," *IEEE Transactions on Microwave Theory and Techniques*, Vol. 67, No. 4, 1308–1315, 2019.
9. Qiu, L. and Q. Chu, "Balanced bandpass filter using stub-loaded ring resonator and loaded coupled feed-line," *IEEE Microw. Wireless Compon. Lett.*, Vol. 25, No. 10, 654–656, 2015.
10. Feng, W., W. Che, and Q. Xue, "Balanced filters with wideband common mode suppression using dual-mode ring resonators," *IEEE Trans. Circuits Syst. I, Reg. Papers*, Vol. 62, No. 6, 1499–1507, 2015.
11. Hong, J. S. and M. J. Lancaster, *Microstrip Filters for RF/Microwave Applications*, Wiley, New York, 2001.